LA-UR -85-1777

CONF-8505166--1
RECEIVED BY OSTI JUN 07 1985

Los Alamos National Laboratory is operated by the University of California for the United States Department of Energy under contract W-7405-ENG-36

TITLE ISOVECTOR RESONANCES IN PION CHARGE EXCHANGE

LA-UR--85-1777

DE85 012746

AUTHOR(S) J. David Bowman

SUBMITTED TO The Proceedings of the Symposium on Nuclear Structure, May 20-24, 1985 for Niels Bohr Hundredth Anniversary.

DISCLAIMER

Los Alamos Los Alamos National Laboratory
Los Alamos, New Mexico 87545

FORM NO 836 R4
ST NO 2629 5/81

ISOVECTOR RESONANCES IN PION CHARGE EXCHANGE *

J. DAVID BOWMAN

Los Alamos National Laboratory
Los Alamos, NM 87545

The $(\pi^{\pm}, \pi^{\circ})$ reactions as probes of isovector resonances are discussed. Experimental observation of the isovector monopole resonance is reported. Experimental results are presented for L=0, 1, and 2 isovector resonances and are compared to random-phase approximation calculations.

Giant resonances are collective excitations of the nucleus in which large numbers of nucleons move collectively. They are simple modes of nuclear excitation that can be interpreted microscopically or macroscopically. Their experimental observation and study as well as their theoretical interpretation are important for models of nuclear excitation and the knowledge of the nucleon-nucleon interaction in the nuclear environment.

In this paper I describe a series of experiments that searched for and studied L=0,1, and 2 isovector electric resonances in the $(\pi^{\pm},\pi^{\circ})$ reactions. The work was done by a collaboration of Los Alamos National Laboratory and Tel Aviv University. A more complete account of the work is available elsewhere .[1] The experimental properties that characterize a giant resonance are the concentration of a large fraction of the total available transition strength with specific quantum numbers in a narrow region of excitation energy, the occurrence of resonances in a wide range of nuclei, and the smooth variation of excitation energy and width of the resonance with nuclear mass A. In contrast to the isoscalar electric modes, which have been extensively studied in the scattering of hadronic probes, the L=1, T=1 or giant dipole resonance (GDR) which has been studied with electromagnetic probes and the L=0, T=1, S=1 Gamow-Teller resonance, which has been studied in the (p,n) reaction, the L=0 T=1 isovector monopole resonance (IVM) and L=2, T=1 isovector quadrupole resonance (IVQ) were poorly characterized when the present work was begun. The study of the IVM was of particular importance. Its existence had been predicted by both macroscopic[2] and microscopic[3] theories, but it had not been observed. The IVM plays a central role in Coulomb effects such as isospin mixing in nuclear ground states, Coulomb displacement energies and widths of analog states.

The quantum numbers and dynamical properties of the pion make the pion charge-exchange reactions $(\pi^{\pm},\pi^{o})$ ideal for the study of electric isovector resonance especially the IVM. First, the observation of a charge-exchange reaction which excites only isovector states eliminates the excitation of isoscalar states which dominate the excitation spectra of inelastic scattering processes.

Second, at forward angles, where the angular distribution of the IVM peaks, pion charge exchange excites primarily electric, or non-spin-flip transitions (in contrast to the (p,n) reaction), reducing spin-flip backgrounds.

Third, the pion is a strongly absorbed probe. The total $\pi^{+}p$ reaction cross section at the peak of the (3/2,3/2) resonance(165 MeV=T) is 200 mb. The strong absorption of the pion is essential for the excitation of a monopole state for which the radial integral of the transition density is zero. The angular distributions produced by the surface related diffractive pion scattering process (similar to (α, α)) oscillate sharply and characteristically with angle.[4]

$$\frac{d\sigma}{d\Omega} \sim J_0^2 (kR\theta) \text{ for } L = 0$$

$$\frac{d\sigma}{d\Omega} \sim J_1^2 (kR\theta) \text{ for } L = 1$$

$$\frac{d\sigma}{d\Omega} \sim J_0^2 (kR\theta) + 3J_2^2 (kR\theta) \text{ for } L = 2$$

where k is the π momentum, θ is the scattering angle and R is the strong absorption radius. This oscillatory behavior serves to identify the multipolarity of the transition and to distinguish the giant resonance signals from the nonresonant background. In Fig. 1 representative angular distributions for the ^{90}Zr (π^{-},π^{o}) reaction at 165 MeV are shown. The qualitative patterns of the angular distributions do not depend on the details of the reaction model used so long as the pion waves are strongly absorbed.

Fourth, the Coulomb energy shift for states populated by the (π^{-}, π^{o}) reaction is advantageous. This point is illustrated in Fig. 2 where the analog state relations are shown for an isovector resonance built on a target ground state of isospin T. For nuclei with T>>1 transitions to the state of lowest total isospin are strongly favored by isospin coupling coefficients. The state of total isospin T+1 in the (π^{-},π^{o}) daughter is shifted down by the Coulomb

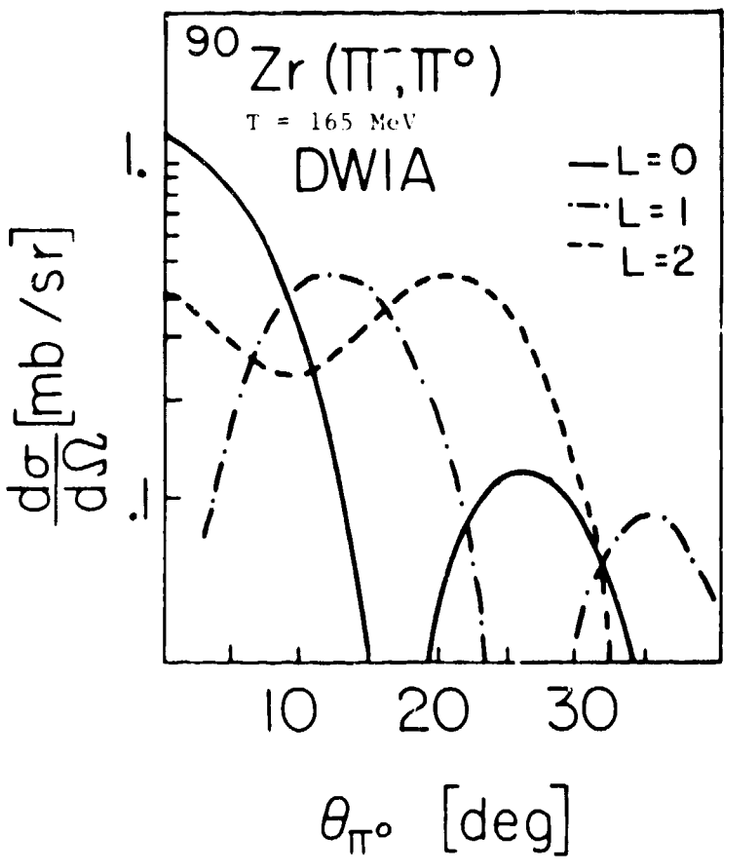

Fig. 1 DWIA calculations of pion charge exchange angular distributions at 165 MeV for L=0,1,2 giant resonances. The shapes resemble the diffractive Bessel function relations. Note that the L=0 and L=2 angular distributions are clearly distinguishable.

displacement energy relative to its analog in the parent nucleus. Thus the T + 1 state has a relatively low excitation energy in the (π^-,π^0) daughter and occurs at an excitation energy where the density of states of the same isospin is small. The opposite situation pertains for the (π^+,π^0) reaction. The T + 1 component populated in the (π^-,π^0) reaction is expected to be narrow and to occur at a low excitation energy while the T-1 component populated in the (π^+,π^0) reaction is expected to be wide and to occur at a high excitation energy. Of course the observation of the isospin splitting of resonances is interesting and is possible if the T-1 component is not too wide.

The experiments described here were carried out at the Clinton P. Anderson Meson Physics Facility in Los Alamos, New Mexico (LAMPF). LAMPF and other meson factories provide intense monochromatic charged pion beams. The neutral pions were detected with the LAMPF π^0 spectrometer.[5] This spectrometer detects neutral pions with a solid angle of ~1msr, an energy resolution as small as 2

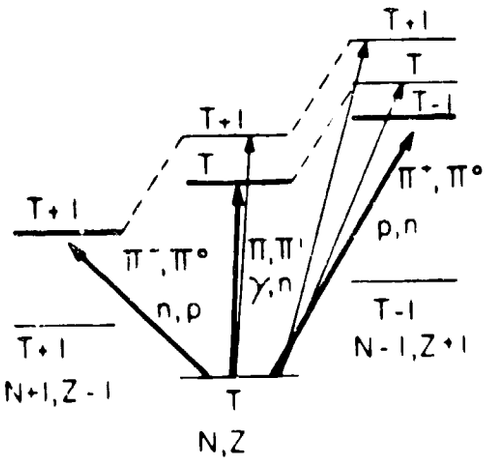

Fig. 2 Isospin allowed transitions for isovector resonances. The dashed lines connect states of the same isospin multiplet. For neutron rich targets the tdransitions to the lowest isospin components (thick lines) are favored. In N=Z nuclei (T=0) transitions are allowed only to the T+1 multiplet. Several reactions which may be used to excite these isospin components are listed.

MeV and an angular resolution of a few degrees. The principle of operation of the π^o spectrometer is as follows: Neutral pions decay nearly instantaneously into two photons. In the π^o center of mass frame the two photons travel in opposite directions and each has one half the π^o rest energy. In the lab frame the photons are thrown forward and their energies are no longer the same. The relationship between the π^o total energy γm_o and the laboratory variables is

$$\gamma m_o = \sqrt{\frac{2}{(1-\cos\eta)\,(1-X^2)}} \quad ; \quad X = \frac{E_1 - E_2}{E_1 + E_2} \quad ,$$

where m_o is the π^o mass, η is the angle between the two photons and E_1 and E_2 are the energies of the photons. Figure 3 shows the π^o spectrometer schematically. The photons are converted into e^+, e^- pairs in lead glass Cherenkov slab detectors. The shower energy is absorbed in arrays of Cherenkov block detectors. The energy resolution of the Cherenkov detectors is 30% at 100 MeV, too broad for nuclear physics work. The π^o energy determination is based on a good measurement of the opening angle η using multi-wire proportional chambers to detect the charged particles emerging from the slab converters. Since X enters into the expression for the π^o energy in second order, good π^o energy resolution can be obtained by selecting events with small X values.

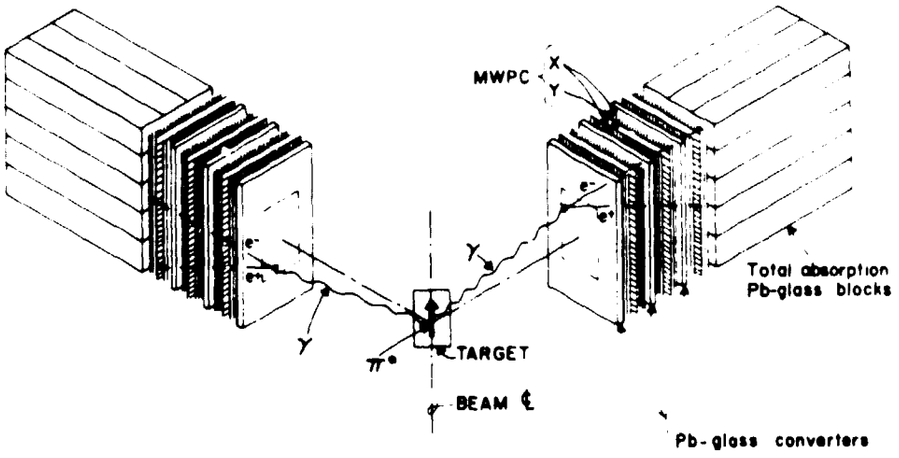

Fig. 3 Schematic diagram of the LAMPF π^{o} spectrometer.

In the experiments ^{40}Ca, ^{60}Ni, ^{90}Zr, ^{120}Sn, ^{140}Ce, and ^{208}Pb, targets were bombarded with 165 MeV $\pi^{\pm}$ beams. Neutral pions were detected and double differential cross sections were determined for angles between 0 and 33^{o} and for π^{o} energies between 90 and 180 MeV. Similar data were taken for ^{40}Ca, ^{60}Ni, and ^{120}Sn targets at $\pi\pm$ energies of 230 MeV. Data for the ^{120}Sn target with a 165 MeV π^{-} beam are shown in Fig. 4a and 4b. At the most forward angle, 4.5^{o}, the IVM cross section is expected to be the largest. The second angle, 11^{o}, is chosen to be near the first minimum of the monopole angular distribution. The GDR cross section is small at the forward angle and has a maximum near 11^{o}. Figure 4c shows the results of subtracting the 11^{o} spectrum from the 4.5^{o} spectrum. This subtraction suppresses the approximately isotropic non-resonant background. The IVM signal is the positive-going hump and the small GDR signal is the negative-going hump.

The above analysis shows the existence of peaks in the $\frac{d^2\sigma}{d\Omega dE}$ versus E spectra above an approximately isotropic background. The IVM peak is visible in a comparison of the 4.5^{o} and 11^{o} spectra but the GDR peak is not. The subtraction procedure makes the weak GDR peak visible. To investigate the degree of isotropy of the non-resonant background it is necessary to look at the angular dependence of different regions of excitation energy versus scattering angle or momentum transfer q. In Fig. 5 I show the forward-angle data for ^{60}Ni (π^{-},π^{o}) taken at 230 MeV. As before, the IVM is large in the most forward angle where the GDR is small. The IVM is small at the second angle where the GDR is large and both are small at the largest angle. In general cross sections depend on energy loss ν and momentum transfer q^2. In Fig. 6 I show $d\sigma/d\Omega$ obtained by integrating over the three regions indicated in Fig. 5. Region one emphasizes

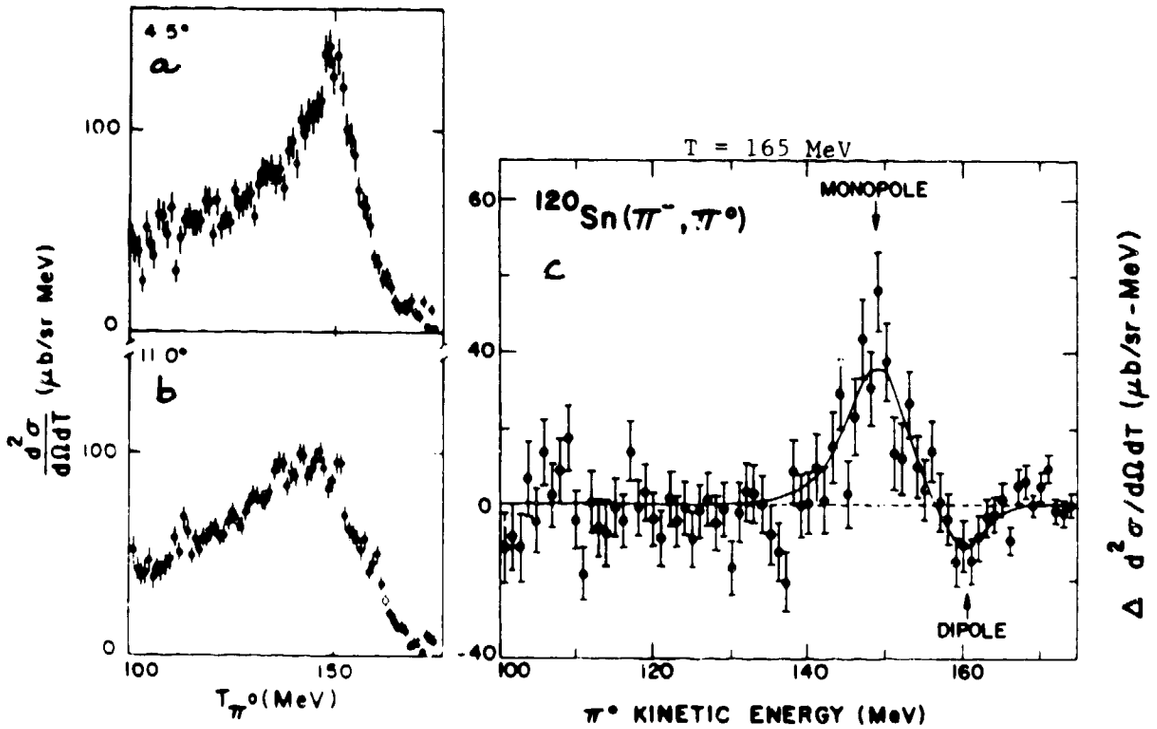

Fig. 4a,b Double differential cross sections in the ^{120}Sn (π^-,π^o) reaction at 4.5^o and 11^o. Figure 4c is the difference of the 4.5^o and 11^o spectra.

the IVM, region two emphasizes the GDR and region three contains mostly nonresonant background.

Each plot can be represented as a superposition of a background linear in q^2 and a component having the q^2 dependence expected for $d\sigma/d\Omega$ for a L=0 or 1 resonance. Although the background is not strictly isotropic its dependence on q^2 is much less rapid than that of the giant resonances. The strongly oscillatory angular distributions of the giant resonances arise from spatial interference of the scattered waves from the widely separated nuclear volume elements. At large excitation energies most of the observed π^o yield results from knocking a nucleon out of the nucleus. At small excitation energies the finite energy acceptance of the π^o spectrometer averages over many overlapping states of different angular momentum. Both these processes result in featureless background angular distributions.

In order to quantitatively extract excitation energies, widths, and maximum cross section, a least-squares fitting procedure was followed. The double differential cross section as a function of q^2 and ν was written as a sum of two Gaussian peaks at an angle-independent excitation energy. The q^2 variation of the peaks was taken to be that of distorted wave impulse approximation calculation using RRA[6] transition densities. The size of the maximum cross

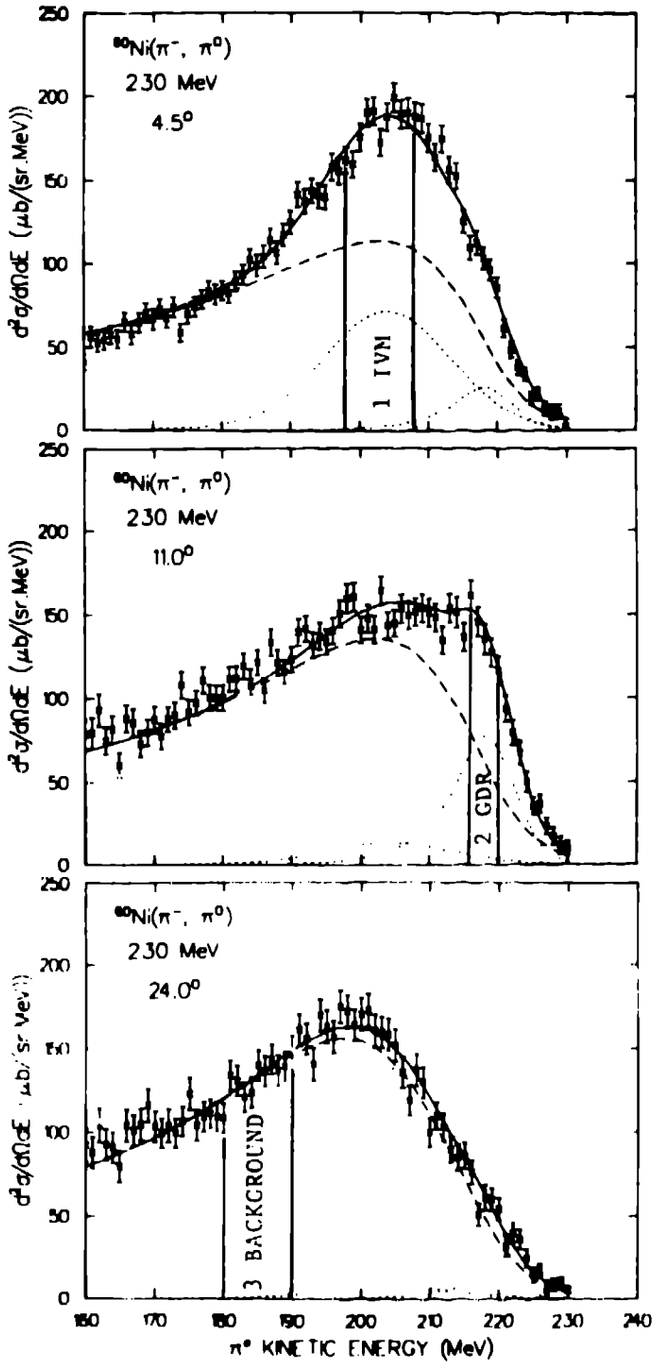

Fig. 5 Double differential cross sections for the ^{60}Ni (π^-,π^0) reaction at three angles.

sections was varied. The background was written as a function having a smooth ν dependence and a quadratic q^2 dependence. Resonance and background parameters were varied to fit the data for each target. The A dependence of the background

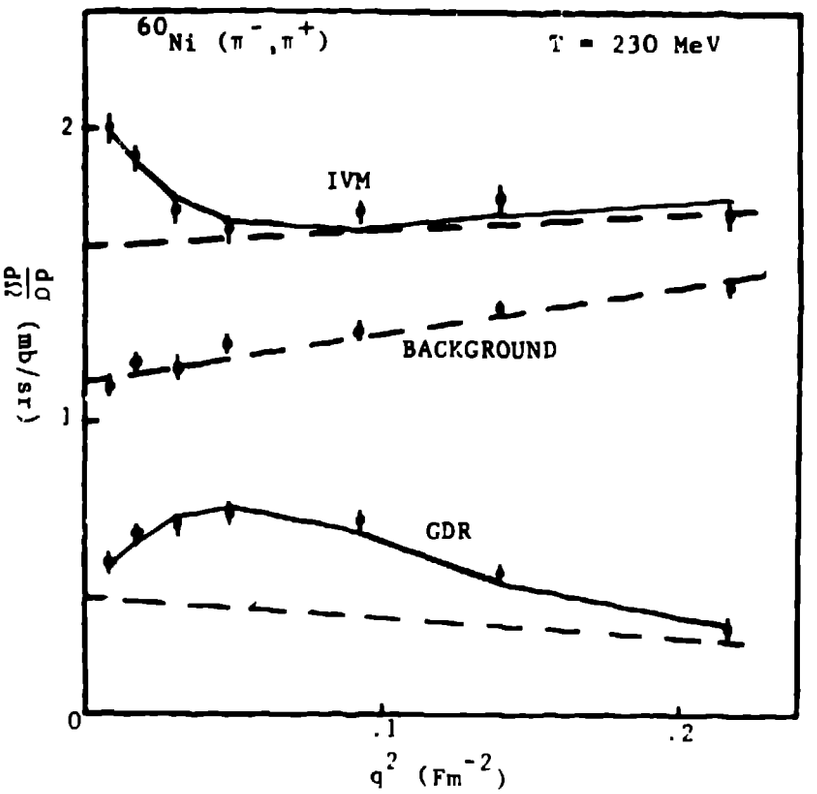

Fig. 6 Differential cross sections for the three regions defined in Fig. 5. The solid lines are fits to the data. The dashed lines are the components linear in q^2. The solid curves are sums of the linear components and components being the q^2 dependence of the IVM and GDR angular distributions.

parameters was found to be a smooth function of A. Furthermore, for targets where data were taken at both 165 and 230 MeV bombarding energy, the extracted resonance energies and widths were consistent although the background shapes were different. The χ^2 per degree of freedom of the fits were between 1.0 and 1.3. The background function and the resonance components shown in Fig. 5 were obtained in this way.

As a further test of the analysis procedure fits were performed as above except that the Bessel function forms for the angular distributions were used with the strong absorption radii treated as free parameters. The results for radii extracted in this way are in good agreement with values obtained from elastic scattering as shown in Fig. 7.

In Fig. 8 and 9 I compare the extracted maximum cross sections, excitation energies, and widths for the IVM and GDR resonances with results of random-phase-approximation distorted-wave-impulse-approximation calculations.[6]

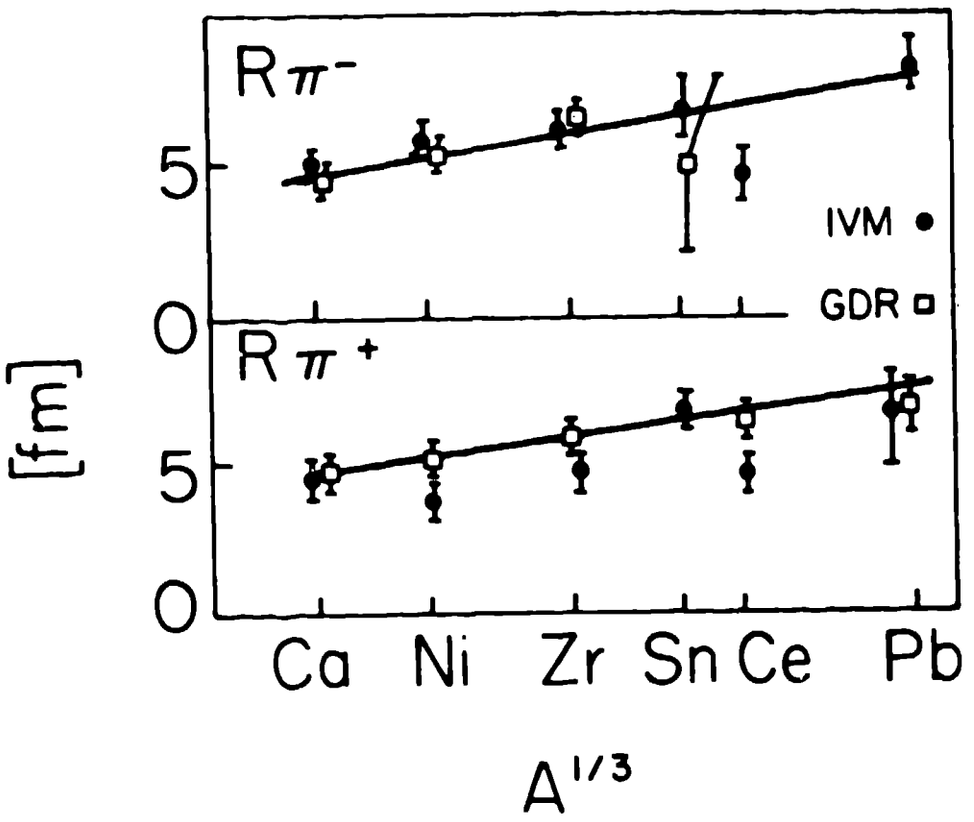

Fig. 7 Interaction radii for IVM and GDR in $(\pi^{\pm},\pi^{o})$ reactions compared with radii from π elastic scattering.

The A dependence of the 1 ħω GDR cross sections can be understood as follows. In the (π^{-},π^{o}) reaction a proton is turned into a neutron and is promoted by one major shell. For the T=0 nucleus, ^{40}Ca, there is no blocking and the π^{+} and π^{-} cross sections are comparable. For ^{208}Pb the neutron shell is fully occupied and the (π^{-},π^{o}) cross section for the GDR is zero. The same effect is seen to a lesser extent for the A dependence of the 2 ħω IVM maximum cross sections. Here the (π^{-},π^{o}) IVM cross sections decrease by about a factor of two from ^{40}Ca to ^{208}Pb while the (π^{+},π^{o}) IVM cross sections are approximately constant. As expected, the widths and excitation energies of T$\not<$1 states are larger than those of the corresponding T+1 states. Where data are available from other reactions, they are also shown. The solid curves give the theoretical results for multipole strength weighting and the dashed curves give the results for cross section weighting. The cross-section-weighted RPA theory using the Skyrme III residual interaction qualitatively describes the data. The excitation energy and widths for the T-1 component of the IVM are somewhat higher then the data, indicating a possible influence of multi-particle-hole

states. If the excitation energy of the isospin $T_<$ component of the IVM in the parent nucleus is estimated using the RPA value of the isospin energy splitting the data fall on the curve

$$E_x T_< = (59.2 \pm 2.6)\ A^{-1/6} \quad ,$$

considerably lower than the hydrodynamical estimate,[2]

$$E_x = 170\ A^{-1/3} \quad .$$

So far nothing has been said about the isovector quadrupole resonance. No IVQ peak was necessary to fit the experimental double differential cross section data. A third Gaussian peak was added to the fitting function. The excitation energy, width, and q^2 dependance of the peak were taken from RPA-DWIA. The data were refitted and 90% confidence level upper limits were deduced for the presence of an IVQ component. These upper limits were 0.18, 0.30, and 0.15 of the RPA-DWIA estimate of the peak IVQ cross section for ^{40}Ca, ^{60}Ni, ^{90}Zr (π^-,π°) respectively. For the IVM and GDR the observed cross sections were typically 0.60 of the RPA-DWIA calculations. Shifting the assumed excitation energies away from the RPA values did not affect the deduced upper limits. If a much larger width was assumed the upper limit for the IVQ cross section was increased and became consistant with the RPA-DWIA estimate.

Isovector quadrupole strength has been observed in the (γ,n) reaction[7] but the extraction of the strength is model dependent. Recently Wright et al.,[8] have searched for the IVQ in the elastic scattering of photons from ^{40}Ca. They conclude that there is less then 0.5 of the energy-weighted sum rule estimate of IVQ strength below 50 MeV excitation energy. Thus two different methods fail to find a compact IVQ resonance. These results pose a problem for microscopic theories of the structure of giant resonances. Perhaps the spreading width (the mixing of multi-particle-hole components into the wave function of these resonances) which is neglected in RPA calculations is important for the IVQ.

Isovector resonances of L=0, 1 and 2 have been studied using the $(\pi^\pm,\pi^\circ)$ reactions. The isovector monopole resonance was found to be a general feature of the excitation spection of nuclei from ^{40}Ca to ^{208}Pb. The T+1 and T-1 isospin components of the isovector monopole and giant dipole resonances were observed. Random phase approximation calculation reproduce the excitation energies and widths of the observed IVM and GDR peaks. Random phase approximate, distorted wave impulse approximation calculations approximately

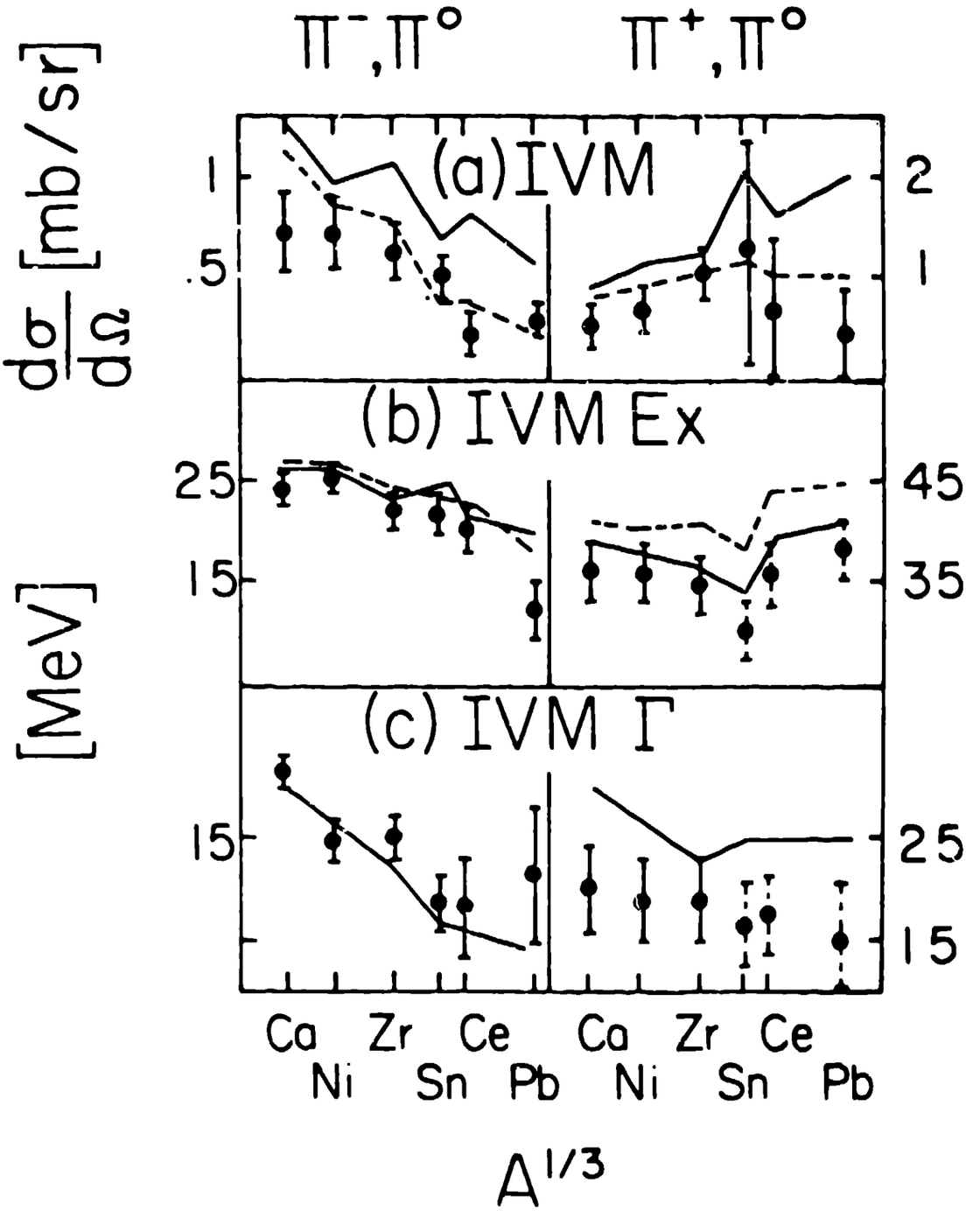

Fig. 8 Maximum cross sections (a), excitation energies relative to the target ground state (b), and widths (c) for the IVM.

reproduce the observed maximum cross sections. No isovector quadrapole strength was observed indicating problems in random phase approximate calculations of this state.

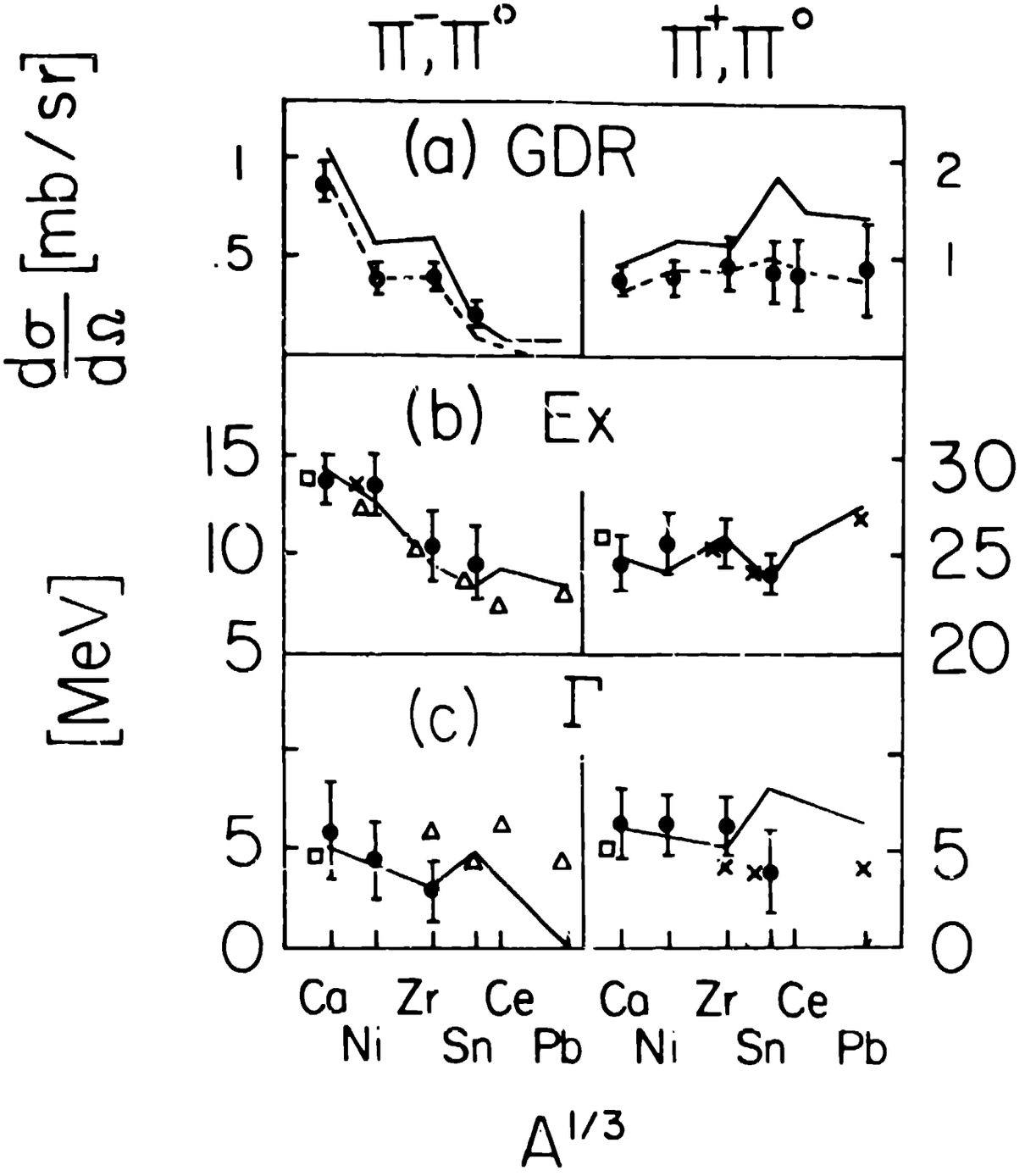

Fig. 9 Maximum cross section (a), excitation energies (b), and widths (c) for the GDR.

*Work was supported by the U.S. Department of Energy and by the U.S.-Israel Binational Science Foundation.

REFERENCES

1. J. D. Bowman et al., Phys. Rev. Lett. 50, 1195 (1983); A. Erell et al., Phys. Rev. Lett. 52, 2134 (1984); A. Erell, PH.D. Thesis unpublished, Tel Aviv University, 1984.

2. A. Bohr and B. R. Mottelson, Nuclear Structure (Benjamin, New York, 1975).

3. G. F. Bertsch and S. F. Tsai, Phys. Rev C18, 125 (1975); K. F. Liu and G. E. Brown, Nucl. Phys. A265, 385 (1976); N. Auerbach, Nucl. Phys. A182, 247 (1972).

4. J. D. Bowman et al., Phys. Rev. Lett. 46, 1614 (1981); A. Gal, Phys. Rev. C25, 2680 (1982).

5. H. W. Baer et al., Nucl. Inst. and Meth. 180, 445 (1981).

6. N.Auerbach and A. Klein, Phys. Rev. C28, 2075 (1983); N. Auerbach and A. Klein, Nucl. Phys. A395, 77 (1983); A. Klein, PH.D. Thesis, Tel Aviv University, 1984.

7. S. S. Hanna et al., Phys. Rev. Lett. 32, 114 (1974); T. W. Phillips and R. G. Johnson, Phys. Rev. C20, 1689 (1979); D. M. Drake et al., Phys. Rev. Lett. 47, 1581 (1981).

8. D. H. Wright et al., University of Illinois, Preprint 1985 (unpublished).